# Furmonertinib is an Oral, Irreversible, Highly Brain-Penetrant Pan-EGFR Mutant Inhibitor with Activity Against Classical and Atypical EGFR Mutations

IASLC 2022 North America Conference on Lung Cancer
SEPTEMBER 23-25, 2022 | CHICAGO, IL, USA

Authors: Luna Musib[1], Marcin Kowanetz[1], Qing Li[2], Huibing Luo[2], Jie Hu[2], Stuart Lutzker[1]
[1]ArriVent Biopharma, Burlingame, CA, USA, [2]Allist Pharmaceuticals, Shanghai, China

## Background

- EGFR (also known as ERBB1, HER1) is comprised of an extracellular domain, a transmembrane domain, and an intracellular tyrosine kinase domain. Mutational activation of EGFR is a common and early event in the development of NSCLC and confers oncogene dependency on the growth and proliferation of the cancer cell.
- EGFR-mutant NSCLC is further divided into those with so-called "classical" activating EGFR mutations (exon 19 deletions and L858R point mutation in exon 21) and those with other activating EGFR mutations (exon 20 insertions), each having different treatment options.
- EGFR-TKIs include first-generation (eg, erlotinib, gefitinib), second-generation (eg, afatinib, dacomitinib), and third-generation (eg, osimertinib) molecules. First generation EGFR-TKIs bind reversibly to EGFR, while second and third generation EGFR-TKIs bind irreversibly to a cysteine (C797) to form a covalent adduct that inhibits EGFR kinase activity.
- Furmonertinib (AST2818) is a potent, orally bioavailable, highly brain-penetrant, third-generation EGFR inhibitor with unique chemical structure designed to improve potency and specificity
- A pharmacologically active metabolite (AST5902) has been identified in the plasma after oral administration of furmonertinib. AST5902 has similar activity and selectivity as furmonertinib and has similar exposure as furmonertinib at clinical doses.
- In studies conducted in China, furmonertinib demonstrated improved PFS in untreated classical EGFR-mutant NSCLC over gefitinib (FURLONG study)[1], improved CNS antitumor activity[2], and promising preliminary clinical activity in patients with EGFR exon 20 insertions[3].
- Furmonertinib is being studied globally in these and other EGFR mutant NSCLC (NCT05364073).

## Methods

- Molecular modeling of furmonertinib and osimertinib in EGFR L858R, D770_N771insNPG, and G719S mutants was performed with Molecular Operating Environment (MOE) software (Chemical Computing Group) using 6JWL, 4LRM, and 2ITN EGFR crystal structures obtained from PDB.
- Kinase selectivity was assessed using a selected panel of 20 kinases under Km ATP conditions by mobility shift assay (Crown Biosciences).
- Furmonertinib in vivo inhibitory activity was tested by cell viability assays in both tumor and Ba/F3 engineered cell lines expressing EGFR mutations and in lung cancer cell lines expressing WT EGFR (Kyinno).
- The in vivo antitumor activity of furmonertinib was assessed in tumor xenograft models of classical EGFR mutant (PC-9), EGFR exon 20 insertion patient-derived xenograft (PDX), and Ba/F3 cells expressing EGFR exon 20 insertions, HER2 exon 20 insertions, and G724S mutation (Kyinno).
- A PC-9 luc brain orthotopic study was conducted in mice to evaluate the efficacy of furmonertinib for brain tumors (Wuxi Apptec).
- A single dose mice PK study was conducted over a range of furmonertinib doses (10, 20, 50, and 75 mg/kg). Brain tissue and plasma was collected at serial time points for analysis of furmonertinib and AST5902 concentrations. Brain tissue was perfused to reduce blood contamination, homogenized, and assayed for furmonertinib and AST5902. Brain PK and plasma PK were assessed to determine the brain/plasma partition (Kp) for furmonertinib and AST5902 (Medcillion).
- Free fraction of furmonertinib was measured using ex vivo equilibrium dialysis (Frontage Labs).

## Furmonertinib is a Novel Pan-EGFR Mutant TKI

**Furmonertinib (AST2818)**




**Figure 1a. Structure of furmonertinib highlighting the tri-fluoroethoxypyridine (green) and acrylamide (blue). Red dotted circle highlights the demethylation site.**

- Furmonertinib (**Figure 1a**) is a third-generation, pan-EGFR mutant TKI, structurally different from other third-generation TKIs.
- It covalently binds to C797 of EGFR through an acrylamide bond.
- It contains tri-fluoroethoxypyridine group predicted to improve the binding to EGFR kinase domain through interactions with the hydrophobic pocket (Allist unpublished data).
- Demethylation of furmonertinib forms its main metabolite, AST5902, which is predicted to have similar binding properties as parent AST2818.
- Furmonertinib can adapt and bind to several types of mutated EGFR, including classical (eg, L858R) and other activating mutations such as exon 20 insertions and G719S (**Figure 1b**).




**Figure 1b. Molecular models of furmonertinib (magenta) vs osimertinib (light blue) bound to various EGFR mutants. Yellow circle indicates the unique tri-fluoroethoxy side chain of furmonertinib, which has additional contact points with the hydrophobic residues of the pocket of EGFR compared with osimertinib.**

## Results

### Furmonertinib Shows High Selectivity For EGFR, HER2, and HER4 vs. Other Kinases

**Table 1: Furmonertinib and its metabolite AST5902 $IC_{50}$ against selected kinases using mobility shift assay**

| Kinase Panel | $IC_{50}$ (nM) | |
|---|---|---|
| | Furmonertinib | AST5902 |
| ALK | 524 | 519 |
| BLK | 994 | 581 |
| BRK | 949 | >1000 |
| BTK | 144 | 276 |
| EGFR | 1.9 | 6.9 |
| EGFR_L858R | 1.2 | 2.9 |
| EGFR_T790M_L858R | 1 | 0.92 |
| EGFR (del746-750) | 1.1 | 1.6 |
| EGFR (del746-750)/T790M | 0.34 | 1.2 |
| FAK | >1000 | >1000 |
| FLT3 | >1000 | >1000 |
| FLT4 | >1000 | >1000 |
| FGFR1 | >1000 | >1000 |
| HER2 | 9.4 | 16 |
| HER4 | 1.5 | 1.4 |
| IGF1R | 811 | >1000 |
| INSR | >1000 | 588 |
| ITK | 67 | 121 |
| JAK3 | 47 | 92 |
| PDGFRa | >1000 | >1000 |

- In vitro, at clinically relevant concentrations, furmonertinib and its metabolite AST5902 (at concentrations of 0.1 μM) inhibited the activity of EGFR family members, HER2 and HER4, with biochemical half maximal inhibitory concentration ($IC_{50}$) values of ≤16 nM

## Results (cont'd)

### Furmonertinib and its Metabolite AST5902 are Potent Against Classical and Other Activating Mutations

**Table 2: $IC_{50}$ values of furmonertinib and active major metabolite AST5902 against EGFR and HER2 mutations in cell-based assays**

| Mutation Type | Cell Line | Activating Mutation | $IC_{50}$ (nM) | | |
|---|---|---|---|---|---|
| | | | Furmonertinib | AST5902 | Osimertinib |
| WT EGFR | A431 | WT | 162.6 | 273.1 | 471.6 |
| Classical mutations | PC-9 | Ex19Del | 3.3 | 6.1 | 12.9 |
| | H1975 | L858R/T790M | 10 | 18 | 24 |
| EGFR exon 20 insertion mutations | Ba/F3 | H773_V774insNPH | 88 | 150 | 331 |
| | | V769_D770insASV | 81 | 126 | 321 |
| | | D770_N771insSVD | 48 | 100 | 214 |
| | | D770_N771insNPG | 31 | 49 | 112 |
| Other activating mutations | Ba/F3 | G719S | 12.4 | 11.3 | 55.4 |
| | | S768I | 21.6 | 20.7 | 85.5 |
| | | G724S | 21.3 | 24.8 | 73 |
| | | E709H | 31.3 | 46.3 | 123.6 |
| | | L747S | 15.0 | 13.4 | 37.8 |
| | | E709V | 14.3 | 15.4 | 47.6 |
| | | L747V | 31.6 | 27.1 | 53.7 |
| | | E709-710>D | 89.6 | 95.8 | 197.4 |
| | | E709A | 17.9 | 18.2 | 64.2 |
| | | L861Q | 3.8 | 5.5 | 24.56 |
| HER2 exon 20 insertion mutations | Ba/F3 | ERBB2 A775_G776ins YVMA | 118 | 285 | 489 |
| | | ERBB2 V777_G778ins GC | 25 | 34 | 77 |

- In cell viability assays, furmonertinib and AST5902 shows improved potency for classical and other activating EGFR mutations over osimertinib and HER2 exon 20 insertion mutations.
- Furmonertinib and AST5902 demonstrates lower potency against tumor cells with WT EGFR compared to mutant EGFR.

### Furmonertinib Shows Marked Tumor Growth Inhibition in Human Lung Cancer Xenograft Models

**Figure 2a: Antitumor activity of furmonertinib (AST2818) and AST5902 (major metabolite) in mouse xenograft model of human lung cancer PC-9 expressing EGFR exon 19 deletion in nude mice**

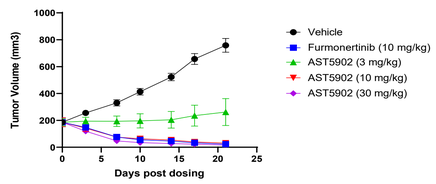


- Furmonertinib (AST2818) at 10 mg/kg QD, (human equivalent dose of ~20 mg QD) inhibited the growth of nude mice subcutaneous xenografts of human lung cancer PC-9 expressing EGFR exon 19 deletion, resulting in complete tumor regression.
- AST5902 (3, 10, 30 mg/kg QD) dose-dependently inhibited the growth of nude mic. subcutaneous xenografts of human lung cancer PC-9-expressing EGFR exon 19 deletion, resulting in partial or complete tumor regression (**Figure 2a).**
- The antitumor effects of AST5902 (10 mg/kg QD) administered alone on PC-9 was comparable to that of AST2818 (10 mg/kg QD) administered at the same dose level.
- Furmonertinib and AST5902 were well tolerated in tumor bearing mice.

**Figure 2b: Antitumor activity of furmonertinib in PDX model LU0387, harboring EGFR exon 20 insertion mutation (H773_V774insNPH)**

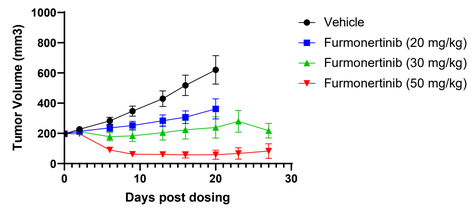


- Furmonertinib 20, 30 and 50 mg/kg QD, (equivalent to human doses of ~ 80, 160, and 240 mg QD based on matching plasma exposures) treatment of HuPrime® LU0387 in a PDX model harboring EGFR exon 20 insertion (H773_V774insNPH) resulted in marked tumor regression in a dose dependent manner (**Figure 2b**).
- Significant tumor regression was observed in the 50 mg/kg QD group (tumor growth inhibition [TGI], 132.5 %) as well as in the 20 and 30 mg/kg QD groups, with TGIs of 61.0 % and 90.2 %, respectively.
- Body weight loss was <10% (not shown) showing that furmonertinib was well tolerated at these doses in mice.

### Furmonertinib Shows Marked Tumor Growth Inhibition in Ba/F3 Cell Lines Harboring Other EGFR Activating Mutations and HER2 Exon 20 Insertion Mutation

**Figure 3a: Antitumor activity of furmonertinib in Ba/F3 subcutaneous tumor model harboring EGFR exon 20 insertion mutation (EGFR V769_D770insASV)**

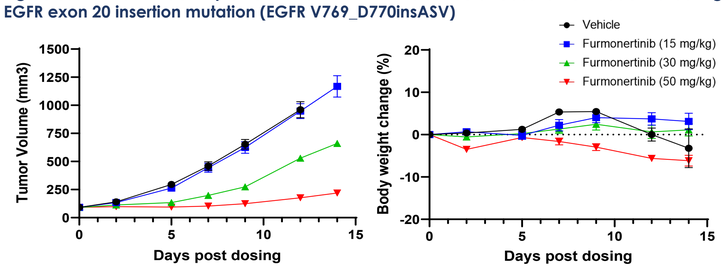


- Furmonertinib oral dosing of 15, 30, and 50 mg/kg QD (human equivalent doses of ~ 40, 160, and 240 mg QD) in a Ba/F3 tumor xenograft model harboring EGFR V769_ D770insASV mutation resulted in tumor regression with minimal change in body weight (**Figure 3a**).

**Figure 3b: Antitumor activity of furmonertinib in a Ba/F3 subcutaneous tumor model harboring G724S activating mutation**

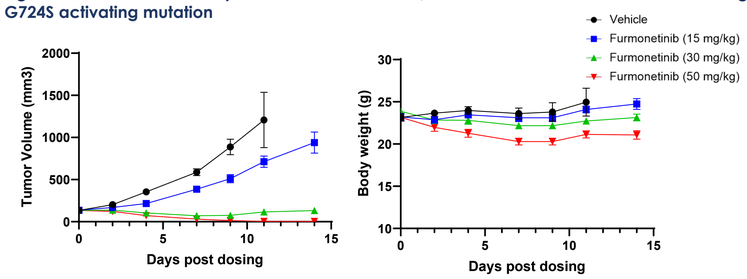


- Furmonertinib oral dosing of 15, 30, and 50 mg/kg QD (human equivalent doses of ~40, 160, and 240 mg QD) in the subcutaneous Ba/F3 G724S mutation xenograft model in female BALB/c nude mice shows marked TGI in a dose dependent manner (**Figure 3b**).

## Results (cont'd)

**Figure 3c: Antitumor activity of furmonertinib in Ba/F3 subcutaneous tumor model harboring HER2 exon 20 insertion mutation (ERBB2 A775_G776insYVMA)**

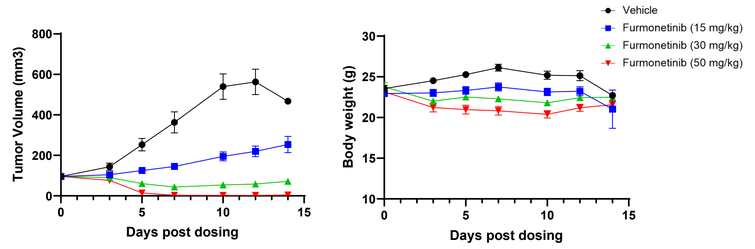


- The in vivo antitumor efficacy of furmonertinib was evaluated in the subcutaneous Ba/F3 ERBB2-V777-G778insGC mutation xenograft model in female BALB/c nude mice.
- Furmonertinib doses of 15, 30, and 50 mg/kg QD (human equivalent doses of ~40, 160 and 240 mg QD) demonstrated significant TGI that was dose dependent (**Figure 3c**).
- Furmonertinib in this model was well tolerated with minimal changes in body weight.

### Once Daily Treatment with Furmonertinib Results in Sustained Inhibition of EGFR in Tumor Xenograft Studies

**Figure 4: Western Blot analysis of tumor tissue lysate from Ba/F3 tumors harboring EGFR exon 20 insertion (V769_D770insASV) collected 1, 4, and 24 hours after 14 days of daily treatment with furmonertinib**

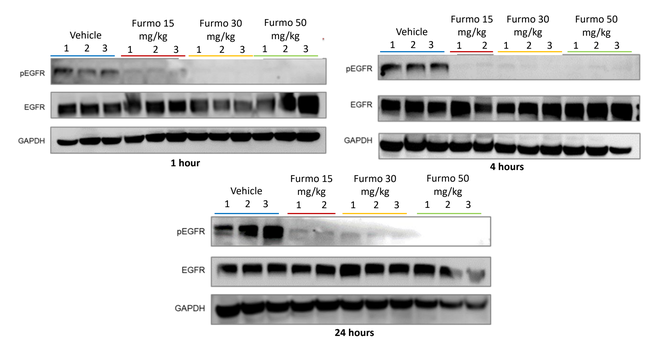


- EGFR phosphorylation in tumors were measured post last dose at serial timepoints, and shows sustained inhibition at all doses tested, supporting once a day dosing.
- Similar results were obtained for the other tumor xenograft studies.

### Furmonertinib Demonstrates High Brain Penetration in Mice PK Study

- Furmonertinib and its metabolite AST5902 are not substrates for P-gp (efflux transporter) in nonclinical studies (data not shown)
- Based on AUC in brain and plasma, the brain plasma ratio (Kp) shows that furmonertinib has high brain penetration (**Table 3**); the active metabolite also has Kp >0.5 indicating good brain penetration as well.
- Brain/plasma ratio of unbound brain and plasma concentrations (Kp,uu) also shows good uptake in brain (**Table 3**), thus supporting efficacy observed in brain orthotopic model (**Table 4**); furmonertinib has 4 times higher Kp,uu than Osimertinib, based on published data.

**Table 3: Brain uptake of furmonertinib and its metabolite based on single dose mice PK study compared to osimertinib**

| Drug | Species | Brain/Plasma Ratio (Kp) | Kp,uu |
|---|---|---|---|
| Furmonertinib | Mice (Balb/c nude) | 3.31 | 0.87 |
| AST5902 (Active metabolite) | | 0.76 | 0.14 |
| Osimertinib | Nude mice | 1.8[a]/2.8[b] | 0.21[c] |

[a] Clin Cancer Res. 2016 Oct 15;22(20):5130-5140.
[b] Tested at 5mg/kg and 25 mg/kg in female SCID mice)
[c] Clin Cancer Res (2021) 27 (1): 189–201.

### Furmonertinib Shows Potent Antitumor Activity in PC-9 Luc Brain Orthotopic Model

- The in vivo efficacy of furmonertinib in the brain was evaluated in the PC-9-Luc EGFR exon 19 deletion orthotopic transplantation tumor model.
- Furmonertinib at 10 and 30 mg/kg QD had significant antitumor effect compared with the vehicle control group (**Table 4**).

**Table 4: Furmonertinib shows dose-dependent activity in PC-9-Luc orthotopic cell transplantation tumor model (based on the bioluminescence signal value on Day 10 after administration)**

| Group | Human Equivalent dose (mg) | Bioluminescent signal (photon/second)[a] (Day 10) | T/C[b] (%) | TGI[b] (%) | p-value[c] |
|---|---|---|---|---|---|
| Vehicle | - | 3.998E + 09 ± 6.644E + 08 | - | - | - |
| Furmonertinib (10 mg/kg) | 20 mg[e] | 4.326E + 08 ± 1.268E + 08 | 10.82 | 90.20 | 0.014 |
| Furmonertinib (30 mg/kg) | 160 mg[e] | 2.400E + 07 ± 4.996E + 06 | 0.60 | 100.49 | 0.010 |
| Osimertinib (10 mg/kg) | 160 mg[d] | 7.544E + 07 ± 3.128E + 07 | 1.89 | 99.19 | 0.010 |

C = mean bioluminescence intensity at the set time in the vehicle control group; T = mean bioluminescence intensity value at the set time in the dosing group; T/C = tumor/control; TGI = tumor growth inhibition.
[a] Mean ± SEM, n = 6
[b] Tumor growth inhibition is calculated by T/C and TGI (TGI [%] = [1- (T10-T0) (V10-V0)] × 100).
[c] p values are calculated from bioluminescent signal values.
[d] Based on matching plasma exposures in mice at 10 mg/kg (Ballard et al. Clin Cancer Res 2016;22(20):5130-40) and human plasma AUC at clinical doses (Jänne et al. N Engl J Med 2015;372:1689-99).

- The mean survival times of the furmonertinib groups at 10 and 30 mg/kg were 28 and 37 days, respectively, and were significantly higher than those of the vehicle control group, which had a mean survival time of 12 days (not shown).

## Summary and Conclusions

- Furmonertinib and its active metabolite AST5902 contain a novel tri-fluoroethoxypyridine group which based on molecular modeling improves interaction with the hydrophobic residues of the pocket in the EGFR kinase domain across different EGFR mutants.
- Furmonertinib exhibits broad pan-EGFR mutant activity against both classical and other EGFR activating mutations, as well as HER2 exon 20 insertion mutations in both cell lines and xenograft models.
- Furmonertinib exhibits high brain penetration and effectively treats EGFR-driven brain metastases in an animal model.
- Activity of furmonertinib is currently being investigated in NSCLC patients with various EGFR activating mutations in global clinical trials (NCT05364073).

## References

- Shi Y, et al. Furmonertinib (AST2818) versus gefitinib as first-line therapy for Chinese patients with locally advanced or metastatic EGFR mutation-positive non-small-cell lung cancer (FURLONG): a multicentre, double-blind, randomised phase 3 study. Lancet Respir Med (2022) Jun 2:S2213-2600(22)00168-0. PMID: 35662408.
- Shi Y, et al. Central nervous system efficacy of furmonertinib (AST2818) versus gefitinib as first-line treatment for EGFR-mutated NSCLC: results from the FURLONG study. J Thorac Oncol. 2022 Aug 3:S1556-0864(22)01496-4. Epub ahead of print. PMID: 35932953.
- Han et al, Preclinical and preliminary clinical investigations of furmonertinib in NSCLC with EGFR exon 20 insertions (20ins). Annals of Oncology (2021) 32 (suppl 5): S949-S1039.

ARRIVENT

ALLIST